Synthesis of highly stable graphite-encapsulated metal (Fe, Co, and Ni) nanoparticles

Seung Jae Lee, Jongjin Jung, Mi Ae Kim, Yong-Rok Kim & Joung Kyu Park

Journal of Materials Science
Full Set - Includes `Journal of Materials Science Letters'

ISSN 0022-2461
Volume 47
Number 23

J Mater Sci (2012) 47:8112-8117
DOI 10.1007/s10853-012-6706-6

Springer

J Mater Sci (2012) 47:8112–8117
DOI 10.1007/s10853-012-6706-6

Synthesis of highly stable graphite-encapsulated metal (Fe, Co, and Ni) nanoparticles

Seung Jae Lee · Jongjin Jung · Mi Ae Kim · Yong-Rok Kim · Joung Kyu Park

Received: 26 April 2012 / Accepted: 30 June 2012 / Published online: 18 July 2012

Abstract Graphite-encapsulated metal magnetic nanoparticles have been attracted for biological applications because of their high magnetization of the encapsulated particles. However, most of the synthetic methods have limitations in terms of scalability and economics because of the demanding synthetic conditions and low yields. Here, we show that well-controlled graphite-encapsulated metal (Fe, Co, and Ni) nanoparticles can be synthesized by a hydrothermal method, simply by mixing metal source with sucrose as a carbon source. The saturation magnetization (Ms) values of Fe/C, Co/C, and Ni/C were 86.6, 43.8, and 113.1 emu/g, respectively. The Fe/C and Ni/C showed higher Ms values than bulk Fe_3O_4 (75.5 emu/g). The graphite-encapsulated metal nanoparticles showed good stability against acid and base environments.

Introduction

Metal and metal-alloy magnetic nanoparticles are of great interest for many applications such as in catalysis for organic synthesis, for removing contaminants from wastewater, as devices for magnetic data storage, for use in biomedicine (e.g., hyperthermia and drug delivery), and as MRI contrasting agents [1–6]. These magnetic nanoparticles combine the beneficial magnetic properties of the core metal or metal-alloy with possible functionalization of the surface. Recently, because of their high magnetization, metal magnetic nanoparticles, such as Fe, Co, and Ni are of interest among several research groups [7–9]. The main problems in the use of pure metals are their instability toward oxidation in an air atmosphere and their tendency to decompose in acid. Moreover, metal nanoparticles have high surface energy that facilitates the agglomeration of the metal particles. Solving these problems is highly important to use these metal nanoparticles in a variety of applications in various fields. Several research groups have focused on developing methods for improving the chemical and physical stabilities of the metal nanoparticles. In order to obtain much higher magnetic moments of the metal magnetic nanoparticles and increase stability, the magnetic core could be protected by an additional surface coating that is chemically inert in air and acids, as well as stable at elevated temperatures. In practice, shell materials such as polymer, silica, or carbon are often used [10, 11]. Presently, several studies are focused on developing carbon shells because of carbon's much higher stability under various physical and chemical conditions such as air, high temperature, and in acid or base solutions. Graphitic carbon encapsulation has been achieved by the electrical arc-discharge technique [12, 13], and by pyrolysis of non-graphitizing carbon materials [14]. However, these synthetic methods have limitations in terms of scalability and economics because of the demanding synthetic conditions and generally low yields. In this paper, we report the development of graphite-encapsulated metal (Fe, Co, and Ni) nanoparticles by a hydrothermal method with a metal source and sucrose as a carbon source. Moreover, the synthesized graphite-encapsulated metal nanoparticles were studied to determine their acid (HNO_3) and base (NaOH) stability by X-ray diffraction analysis.

S. J. Lee · J. Jung · M. A. Kim · J. K. Park (✉)
Research Center of Convergence Nanotechnology, Division of Fusion Chemistry, Korea Research Institute of Chemical Technology, Daejeon 305-600, Korea
e-mail: parkjk@krict.re.kr

S. J. Lee · Y.-R. Kim
Department of Chemistry, Yonsei University, Seoul 120-747, Korea

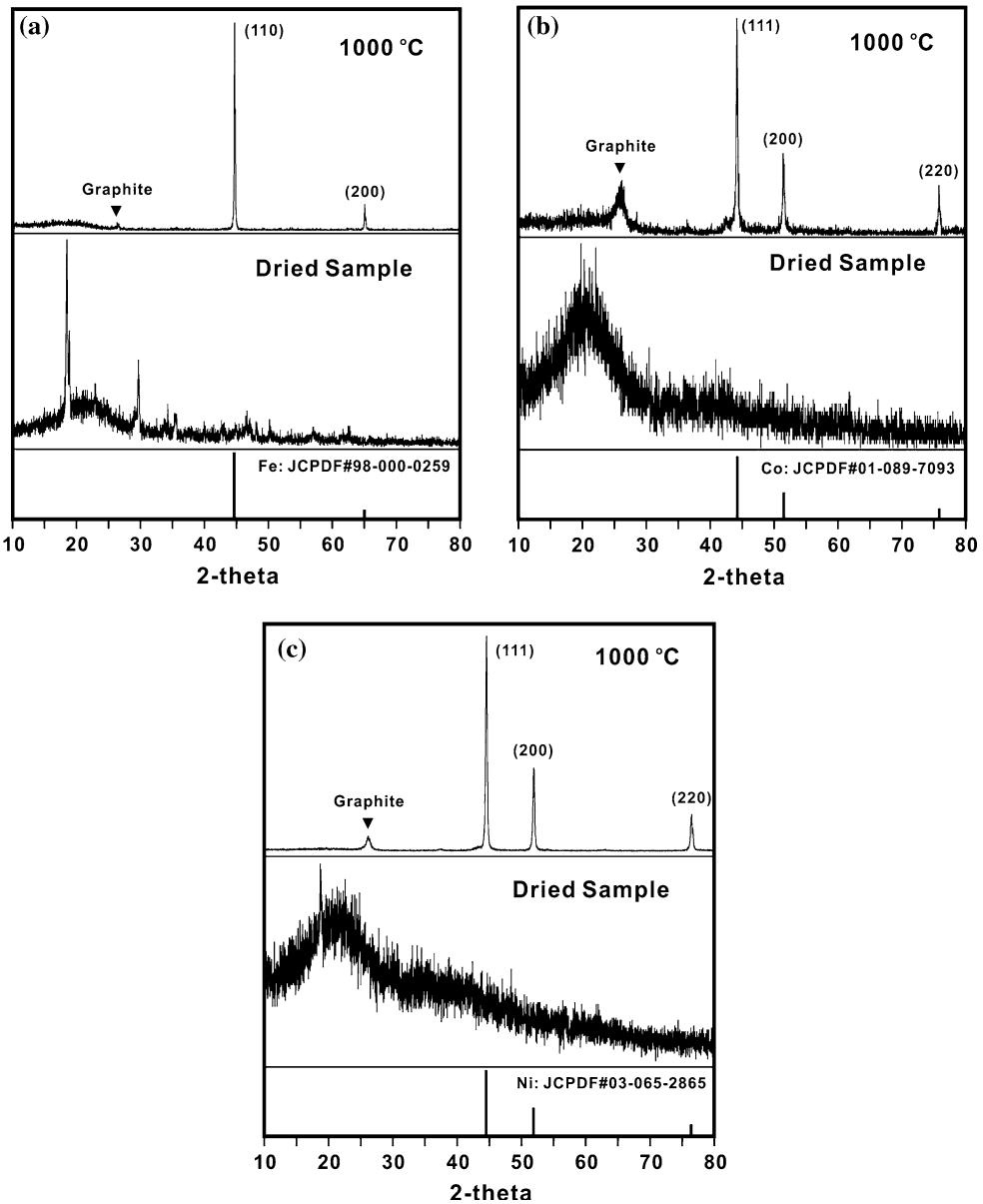

Fig. 1 The XRD patterns of graphite-encapsulated metal nanoparticles: **a** Fe/C. **b** Co/C. **c** Ni/C

Experimental procedure

In a typical experiment, graphite-encapsulated metal core–shell nanoparticles were formed by a simple hydrothermal reaction and a subsequent heat treatment process (Optimum temperatures = 1000 °C). In a typical reaction, a mixture, consisting of metal source ($Fe(NO_3)_3{\cdot}9H_2O$ = 5 mmol, $Co(NO_3)_2{\cdot}6H_2O$ = 5 mmol, and $Ni(NO_3)_2{\cdot}6H_2O$ = 5 mmol) and sucrose ($C_{12}H_{22}O_{11}$ = 8 mmol) as a carbon source, was stirred vigorously to form a clear solution, and then placed in a 45-mL capacity stainless steel autoclave, which was heated in an oven to 190 °C for 9 h. The products were washed several times with distilled water, filtered off, and finally dried in a drying oven at 80 °C for 5 h. Subsequently, the dried products were heat-treated at 1000 °C for 3 h under an Ar atmosphere to grow a graphite shell on the surface of the metal nanoparticles. The hydrothermal treatment at a pressure of 15 bars induces dehydration of the carbohydrate and carbonization, resulting in carbon sources positioned predominantly near the core of the metal (Fe, Co, and Ni) nanoparticles. Consequently, a graphite shell grows on the metal (Fe, Co, and Ni) core during annealing in an Ar atmosphere, resulting in graphite-encapsulated metal (Fe, Co, and Ni) core shells. Annealing of the metal (Fe, Co, and Ni)/C core–shell structures at 1000 °C for 3 h leads to graphite shell growth and highly ordered crystallinity. It seems that the graphite shell minimizes crystal growth and aggregation during this high-temperature annealing [19].

The graphite-encapsulated metal nanoparticles were identified using a Rigaku D/MAX-2200 V X-ray diffractometer using CuKα radiation (λ = 1.5406 Å). Transmission

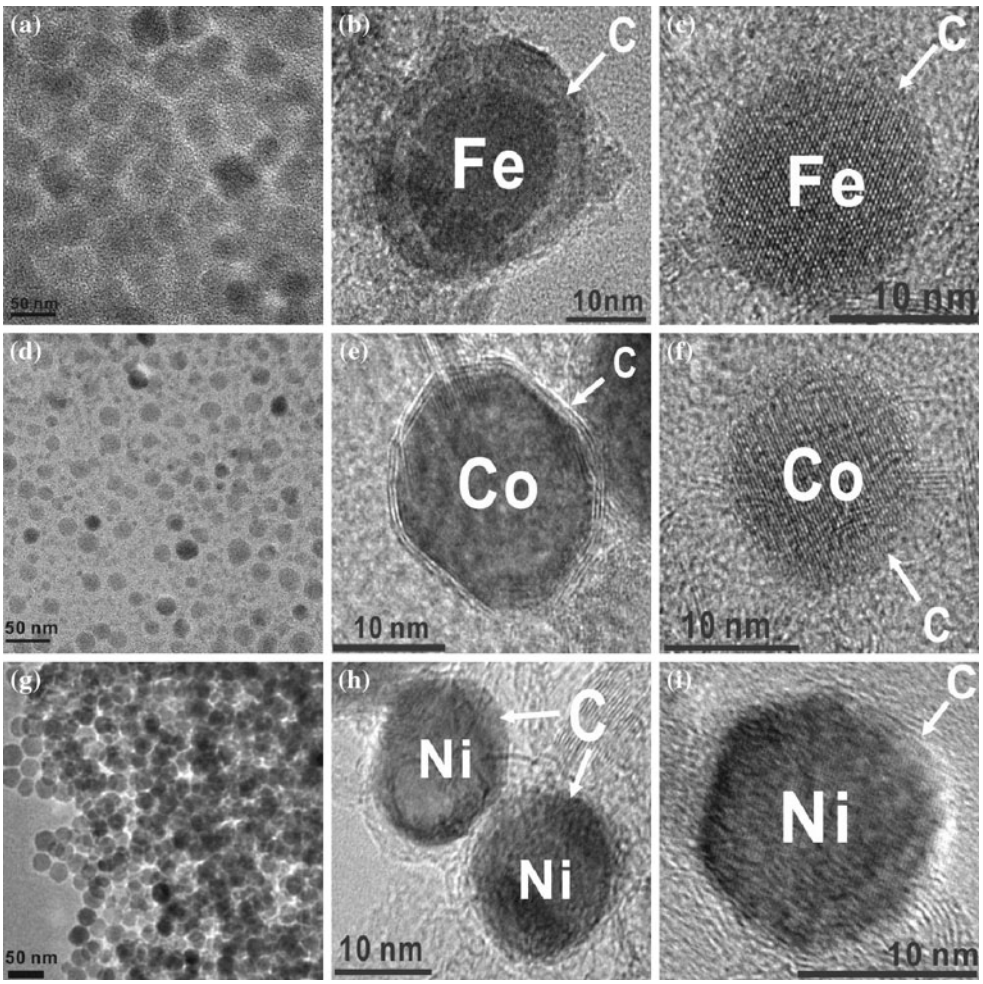

Fig. 2 The TEM images of graphite-encapsulated metal nanoparticles: **a–c** Fe/C. **d–f** Co/C. **g–i** Ni/C

electron microscopy (TEM) and high resolution TEM (HRTEM) images were obtained using a JEM-2100F field emission electron microscope at an accelerating voltage of 200 kV. Samples for TEM were prepared by spreading a drop of the solution samples on copper grids coated with a carbon film followed by drying in the oven at 60 °C. Raman spectroscopic measurement of the metal (Fe, Co, and Ni)/C nanoparticles was carried out using a Senterra Dispersive Raman System (Brucker, Germany) with 632.8 nm. TG spectra of samples were obtained with a TGA Q5000 analyzer under air atmosphere (TA instrument). Magnetic properties were measured on a vibrating sample magnetometer (VSM, Toei Industry Co. Japan).

Results and discussion

The XRD diffraction patterns of the three graphite-encapsulated metal nanoparticles are shown in Fig. 1. For Fe/C, we observed diffraction peaks at $2\theta = 44.66^\circ$ (111) and 65° (200), which are characteristic of Fe (JCPDF # 98-000-0259). Similarly, the structures of the Co/C and Ni/C nanoparticles are also confirmed for Co (JCPDF # 01-089-7093) and Ni (JCPDF # 03-065-2865), as proved by Co (111), (200), and (220) peaks at 44.18°, 51.42°, and 75.8°, respectively; and Ni (111), (200), and (220) peaks at 44.44°, 51.8°, and 76.32°, respectively. The detailed morphology of the graphite-encapsulated nanoparticles was studied by transmission electron microscopy (TEM) (Fig. 2). The low resolution TEM images clearly show spherical type nanoparticles (below 50 nm size, Fe/C: Fig. 2a, Co/C: Fig. 2d, Ni/C: Fig. 2g). The contrast in the micrograph in the TEM image clearly shows that the particles are composed of a metal core and shell. Graphite-encapsulated Fe (Fig. 2b, c), Co (Fig. 2e, f), and Ni (Fig. 2h, i) nanoparticles showed a spherical shape and all nanoparticles were covered by graphite layer. Graphite-encapsulated Fe, Co, and Ni nanoparticles had diameters of about 17.8, 17.4, and 15.6 nm size, respectively, with multi layers; correspondingly, they had diameters of 15.2, 14.3, and 14 nm, respectively, with single layers. The width of

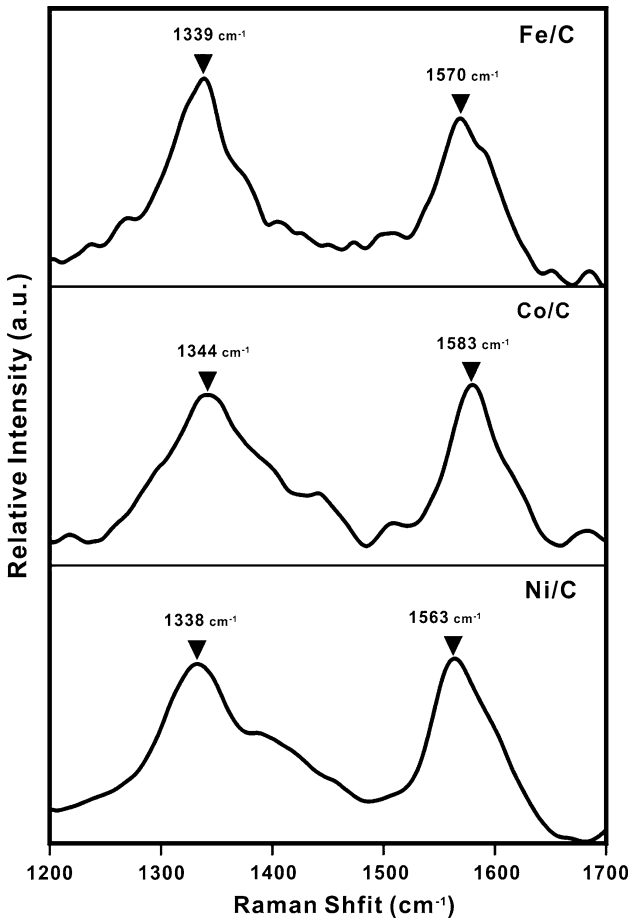

Fig. 3 Raman spectra of graphite-encapsulated Fe, Co, and Ni nanoparticles

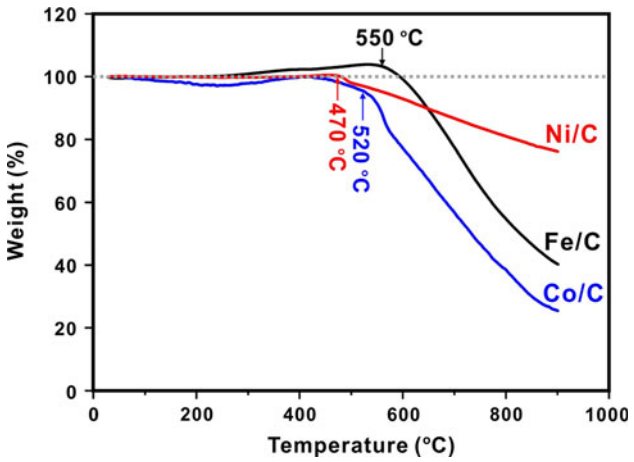

Fig. 4 TGA curves of graphite-encapsulated Fe, Co, and Ni nanoparticles

the diffraction peaks was affected by the average diameter of the nanoparticles. According to the Scherrer equation [15, 20, 21], the average diameter of the nanoparticles yielded around 33.4, 25.5, and 26.3 nm for Fe/C, Co/C, and

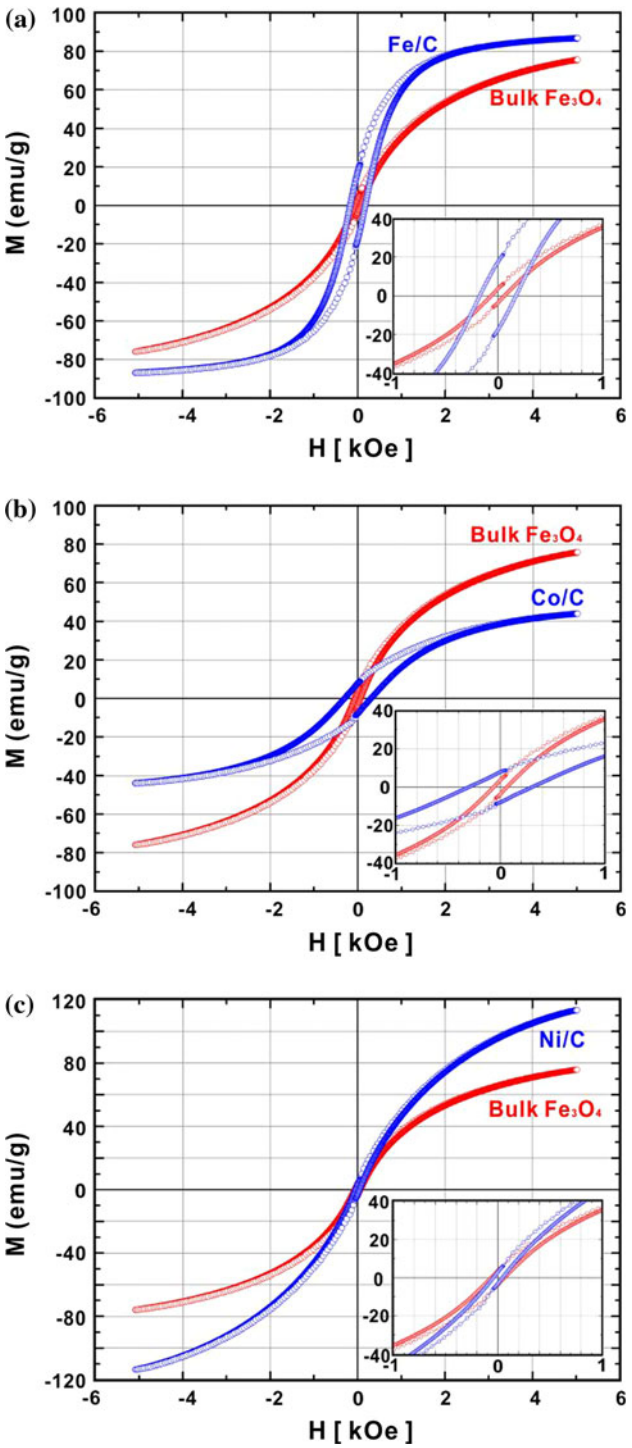

Fig. 5 Hysteresis loops at room temperature of graphite-encapsulated metal nanoparticles: **a** Fe/C. **b** Co/C. **c** Ni/C

Ni/C, respectively. These results agreed fairly well with the results of the TEM, because XRD measures the bulk of the samples whereas the TEM provides information about a finite number of nanoparticles visible in the electron microscope. The diffraction peak at about 26° can be assigned to the (002) planes of the hexagonal graphite

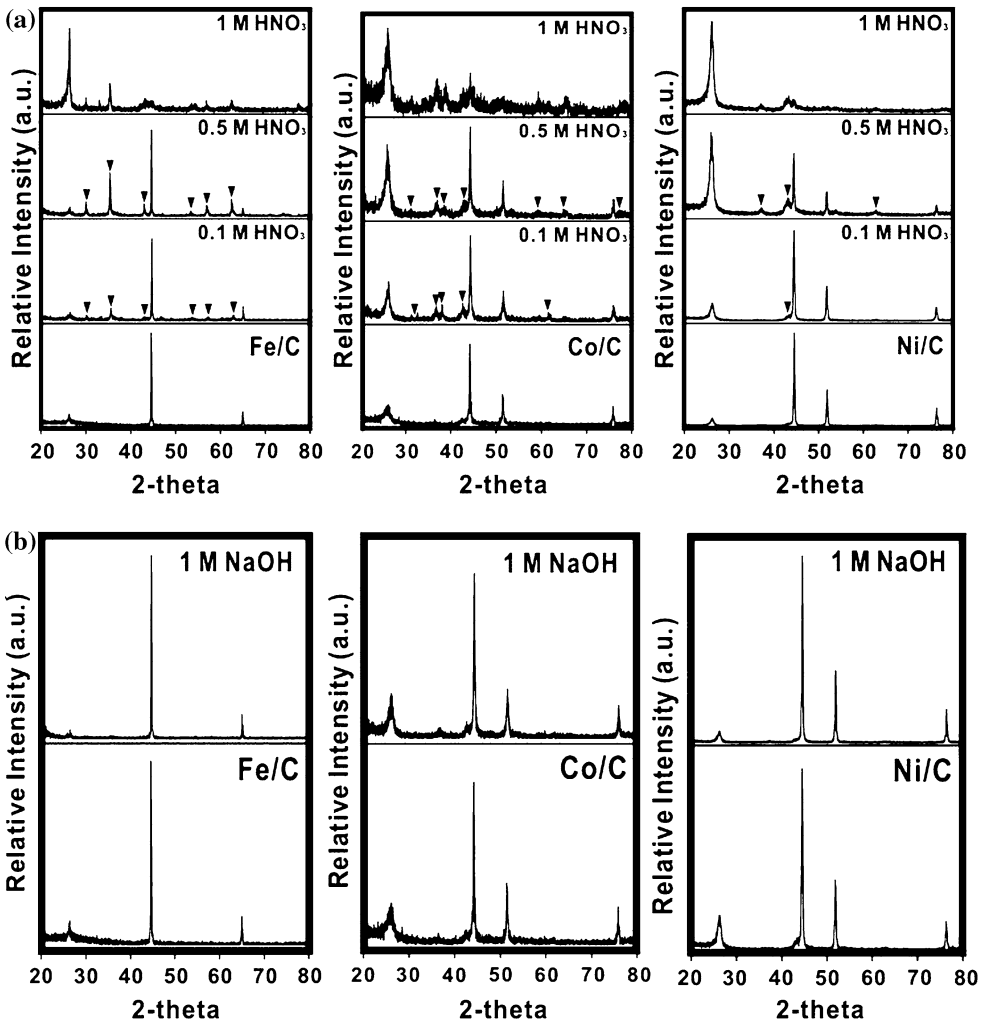

Fig. 6 The XRD patterns of graphite-encapsulated metal (Fe, Co, and Ni) nanoparticles by various environment: **a** Acid (HNO_3). **b** Base (NaOH) solutions

structure, corresponding to the encapsulating graphite shells (Fig. 1); this indicates highly crystalline graphite. Further information about the graphite shell was obtained by Raman spectroscopy (Fig. 3). The two main peaks (Fe/C = 1339 and 1570 cm^{-1}, Co/C = 1344 and 1583 cm^{-1}, Ni/C = 1338 and 1563 cm^{-1}) are in good agreement with the pattern reported for graphite in the literature [16, 17]. The Fe/C nanoparticles have a sharper and stronger D-band (peak around 1339 cm^{-1}) than the Co/C and Ni/C nanoparticles. The D-band of metal/C nanoparticles is considered to be a disorder-induced feature owing to lattice distortion or amorphous carbon background signals [17, 18].

In order to investigate the influence of the graphite shell on thermal stability and oxidation behavior, TGA measurements of the Fe/C, Co/C, and Ni/C nanoparticles were performed at a heating rate of 10 °C min^{-1} in an air atmosphere (Fig. 4). It can be seen that the TGA curves of the Fe/C, Co/C, and Ni/C nanoparticles show weight loss above 550, 520, and 470 °C, respectively, which corresponds to oxidation of the carbon shells to gaseous carbon oxides. The TGA curve of the Fe/C nanoparticles in the range of 255–550 °C revealed a gradual weight gain, which corresponds to oxidation of the un-encapsulated Fe metal nanoparticles. It can be said that these graphite-encapsulated nanoparticles exhibited strong resistance to oxidation with oxygen.

The magnetic properties of the samples were investigated by a vibrating sample magnetometer. The powder sample was packed and the measured weights of the metal nanoparticles were 6 mg. The magnetic moment was measured as a function of magnetic field in the range of −5000 to +5000 Oe at room temperature. Figure 5 shows the full hysteresis loops of the magnetization in an external field for the three metals under study. The quantitative analysis yielded saturation magnetization (Ms) of 75.5, 86.6, 43.8, and 113.1 emu/g for bulk Fe_3O_4, Fe/C, Co/C, and Ni/C, respectively, whereas the remnant magnetization values were 3.9, 17.3, 7.8, and 3.3 emu/g, respectively. The remnant magnetization results indicate that the size distributions of the three samples were different, and that the average size of Fe/C may be larger than those of Co/C and

Ni/C. The Co/C sample showed a large coercive field (Hc) of about 295 Oe, and the Fe/C and Ni/C samples showed Hc of 171 and 43 Oe, respectively.

For the stability test of the graphite-encapsulated metal nanoparticles in acid and base environments, we treated the nanoparticles with varying concentrations of acid (0.1, 0.5, 1 M HNO_3) and base (1 M NaOH) solutions for 7 days at room temperature. Treated samples were washed several times with distilled water and dried in a drying oven at 80 °C for 5 h. We determined the chemical stability in acid and base environments by X-ray diffraction. Sample treated with 1 M NaOH (Fig. 6b) showed typical diffraction peaks for Fe, Co, and Ni metals, indicating that the three samples were not affected by the base environment over 7 days. As can be seen from Fig. 6a, Ni/C exhibited more stability than Fe/C and Co/C in the acid environment. In the 0.1 M HNO_3 solution, the Ni/C nanoparticles showed typical diffraction peaks for Ni metal and small nickel oxide peaks by un-encapsulated Ni metal, that is, 0.1 M HNO_3 did not affect the Ni/C nanoparticles. Ni/C nanoparticles treated with a 0.5 M HNO_3 solution exhibited more Ni metal diffraction peaks than nickel oxide. However, the Ni/C sample-treated 1 M HNO_3 solution showed graphite and nickel oxide diffraction peaks. The Fe/C and Co/C samples treated with 0.1 M HNO_3 showed diffraction peaks of metal and metal oxide. This result indicated that small amount of metals (Fe and Co) were decomposed in 0.1 M HNO_3 environment. However, Fe/C and Co/C nanoparticles showed still good stability in the 0.1 M HNO_3 environment. In the 0.5 M HNO_3 solutions, Fe/C and Co/C nanoparticles showed more metal oxide diffraction peaks, that is, amount of metal oxides were increased more and more for increasing acid concentrations. The metals in the sample were almost decomposed in the 1 M HNO_3 solution. In spite of the decomposition in 0.5 M and 1 M HNO_3 solution, graphite-encapsulated metal nanoparticles showed good stability in 0.1 M HNO_3 after 7 days.

Conclusion

We synthesized graphite-encapsulated metal (Fe, Co, and Ni) nanoparticles by a hydrothermal method, simply by mixing a metal source and sucrose as a carbon source. The saturation magnetization values of Fe/C, Co/C, and Ni/C were 86.6, 43.8, and 113.1 emu/g, respectively. The Fe/C and Ni/C showed higher saturation magnetization values than bulk Fe_3O_4 (75.5 emu/g). In acid (0.1 M HNO_3) and base (1 M NaOH) environments, the graphite-encapsulated metal nanoparticles showed good stability. Graphite-encapsulated metal nanoparticles with high magnetization values and good stability in acid and base environments have potential applications in industry, biological, and environmental fields.

Acknowledgements This study was supported by KRICT general research fund (SI-1210) and the Korean Ministry of Science and Technology (KK-1207-B6). Y.-R. Kim thanks for the support from the Pioneer Research Center Program through the National Research Foundation of Korea funded by the Ministry of Education, Science and Technology (No. 2012-0001066).

References

1. Kong L, Lu X, Bian X, Zhang W, Wang C (2011) ACS Appl Maters Inter 3:35
2. Fuhrer R, Hermann K, Athanassiou EK, Grass RN, Stark WJ (2011) Langmuir 27:1924
3. Tartaj P, Morales MP, Veintemillas-Verdaguer S, Gonzalez-Carreno T, Serna CJ (2003) J Phys D Appl Phys 36:R182
4. Kats E, Willner I (2004) Angew Chem Int Ed 43:6042
5. Huber DL (2005) Small 1:482
6. Lu AH, Salabas EL, Schuth F (2007) Angew Chem Int Ed 46:1222
7. Park JB, Jeong SH, Jeong MS, Kim JY, Cho BK (2008) Carbon 46:1369
8. Liu S-H, Gao H, Ye E, Low M, Lim SH, Zhang S-Y, Lieu X, Tripathy S, Tremel W, Han M-Y (2010) Chem Commun 46:4749
9. El-Gendy AA, Ibrahim EMM, Khavrus VO, Krupskaya Y, Hanmpel S, Leonhardt A, Büchner B, Klingeler R (2009) Carbon 47:2821
10. Gao X, Yu KMK, Tam KY, Tsang SC (2003) Chem Commun 24: 2998
11. Wu M, Zhang YD, Hui S, Xiao TD, Ge S, Hines WA, Budnick JI (2002) J Appl Phys 92:491
12. Ruoff RS, Lorents DC, Chan B, Malhotra R, Subra-Money S (1993) Science 259:346
13. Hayashi T, Hirono S, Tomita M, Umemura S (1996) Nature 381:772
14. Harris PJF, Tsang SC (1998) Chem Phys Lett 293:53
15. Patterson AL (1939) Phys Rev Lett 56:978
16. Nemanich VL, Solin SA (1979) Phys Rev B 20:392
17. Tuinstra F, Koenig JL (1970) J Chem Phys 53:1126
18. Boskovic BO, Stolojan V, Khan RUA, Hap S, Silva SRP (2002) Nat Mater 1:165
19. Lee SJ, Cho J-H, Lee C, Cho J, Kim Y-R, Park JK (2011) Nanotechnology 22:375603
20. Tagarielli VL, Fleck NA, Colella A, Matteazzi P (2011) J Mater Sci 46:385. doi:10.1007/s10853-010-4848-y
21. Bachvarova-Nedelcheva A, Iordanova R, Aleksandrov L, Dimitriev Y, AtaaLLa M (2011) J Mater Sci 46:7177. doi:10.1007/s10853-011-5441-8